Chapter 4

Periodic Orbits

In this Chapter we will see that periodic orbits play a very important role in understanding the behavior of nonlinear dynamical systems. In particular, they determine in large part the structure of strange attractors.

To put the situation into stark perspective, we make the following three observations.

1. If you know everything about all the periodic orbits in a strange attractor, then you know everything there is to know about the strange attractor.

2. If you know a lot about many periodic orbits in the strange attractor, you know a great deal of information about the attractor, and all of the important information.

3. If you know a little bit (the *organization*) about only a few ($2n - 1$, n is the number of letters in the symbol alphabet) of the periodic orbits in a strange attractor, you know most of the important information about the attractor.

We will bring these outrageous claims to life in the course of this Chapter.

4.1   Fixed Points of $f^{(n)}$

In Fig. 4.1 we show plots of $f(x)$ and its first two iterates, $f^{(2)}(x)$ and $f^{(3)}(x)$, of the logistic map for the control parameter value $\lambda = 4$. The important point of these three graphs is that these three functions intersect the diagonal 2, 4, and 8 times. It requires little stretch of the imagination to believe that $f^{(n)}(x)$ has 2^n fixed points.

4.2   Counting Orbits

We can use the information above to count the number of periodic orbits in the logistic map at $\lambda = 4$. This is done as follows. There are two fixed points of
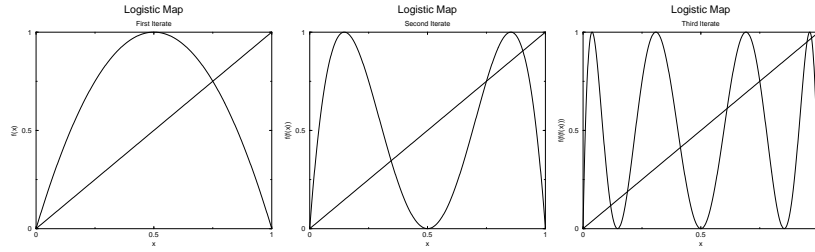
1

Figure 4.1: (a) $f(x)$; (b) $f^{(2)}(x)$; $f^{(3)}(x)$. These functions have 2^n fixed points.

$f(x)$. These are two period one orbits: the fixed point at $x = 0$ and the fixed point at $x = 1 - 1/\lambda$.

The second iterate $f^{(2)}(x)$ has four fixed points. Two of these are the period one orbits. These have *minimal* period one. They can masquerade as period two orbits. Therefore only two of the four fixed points belong to an orbit of minimal period 2. Since there are two such points, and both must be on the same period two orbit, there is only one period two orbit.

The third iterate $f^{(3)}(x)$ has eight fixed points. Two of these are the period one orbits. The period two orbit cannot masquerade as a period three orbit because 2 does not divide three. This leaves $6 = 2^3 - 2 \times 1$ fixed points belonging to two period three orbits. We can now begin to build up a list

p	$N(p)$
1	2
2	1
3	2

This list can be extended recursively. The number of period p orbits is given by

$$N(p) = \frac{1}{p} \left(2^p - \sum_{k \text{ divides } p} k \times N(k) \right)$$

Proceeding in this way, we can quickly build up a list of the number of orbits of period p. This is shown in Table 4.1.

The number of orbits of period p increases exponentially with the period:

$$N(p) \sim e^{p h_T} \tag{4.1}$$

The statistic h_T is the *topological entropy* of the map. We define the topological entropy in general as

$$h_T = \lim_{p \to \infty} \frac{\log N(p)}{p} \tag{4.2}$$

A plot of $\log(N(p))/p$ vs. the period p is shown in Fig. 4.2 (thick curve). It is compared with a plot of $\frac{1}{p} \log(2^p/p) = \log(2) - \frac{1}{p} \log(p)$ (light curve) in

Table 4.1: The number $N(p)$ of orbits of period p is shown for the logistic map at $\lambda = 4$.

p	$N(p)$	p	$N(p)$	p	$N(p)$
1	2	11	186	21	99858
2	1	12	335	22	190557
3	2	13	630	23	364722
4	3	14	1161	24	698870
5	6	15	2182	25	1342176
6	9	16	4080	26	2580795
7	18	17	7710	27	4971008
8	30	18	14532	28	9586395
9	56	19	27594	29	18512790
10	99	20	52377	30	35790267

this graph. The two curves become indistinguishable at around $p = 15$ at the resolution shown. Both approach the limiting value log(2) asymptotically as $p \to \infty$. The topological entropy of the logistic map at $\lambda = 4$ is log(2). We will find simple methods for computing topological entropy below.

4.3   Searching for Periodic Orbits

There are no periodic orbits in a chaotic time series. However, a chaotic time series gets near enough to a periodic orbit from time to time, and while near such an orbit, it behaves very much like that orbit. This allows for the possibility that we can find segments of a chaotic time series which are very similar to some periodic orbits. So similar that they can be treated like unstable periodic orbits for all, or at least most (*i.e.*, all important) practical purposes. Such sections of data from a chaotic time series are called *surrogate* periodic orbits. That is, they can stand in for the unstable periodic orbits which really don't exist in the chaotic time series.

There is a simple procedure for extracting surrogate periodic orbits from a chaotic time series. As typical, we illustrate the method with an example.

Suppose we iterate the logistic map for some value of the control parameter λ which generates a chaotic time series. Throw away the first set of iterates to allow the dynamics to relax to the chaotic attractor. Then save the next N data values $x(1), x(2), \cdots, x(N)$ in a reference library. We look for a low period orbit, of period p, by searching over the data set for the smallest value of

$$diff = |x(i) - x(i + p)|$$

If $diff$ is 'sufficiently small,' we can conclude that a period p orbit exists. The vague term 'sufficiently small' means, as a rule of thumb, that $diff$ is of the
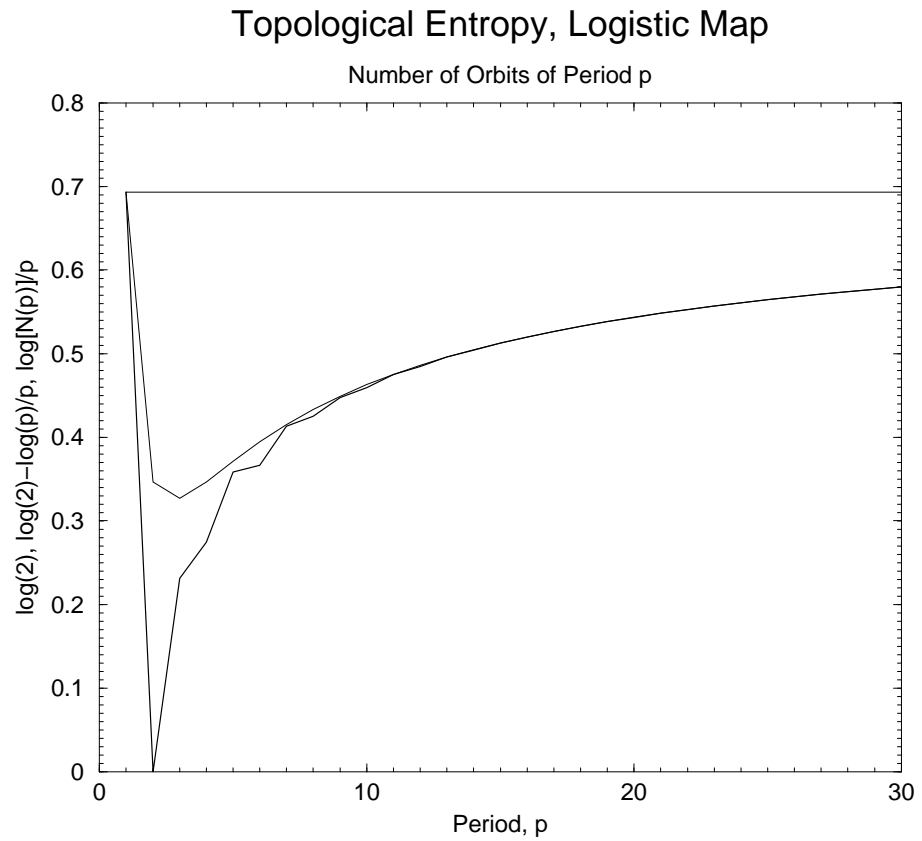
Topological Entropy, Logistic Map

Figure 4.2: The number of orbits of period p increases exponentially with the period, p, in the logistic map. The ratio $\frac{1}{p}\log(N(p))$ (dark curve) approaches $\log(2)$ (horizontal line) as the limit $\log(2) - \frac{1}{p}\log(p)$ (light curve).

order of, or less than, 1% of the 'diameter' of the attractor. The diameter of the attractor can be taken as the largest difference $|x(i) - x(j)|$, over all i, j in the range $1 \leq i, j \leq N$.

There are some subtleties about such searches which have emerged from years of experience. First, it is possible that the period p orbit does not have minimal period p. For example, it might be a period one orbit that 'goes around' p times. Or it could be a period $p/2$ orbit that goes around twice. This isn't possible if p is odd. We use the same test as in the orbit counting problem. We must test that the data values $x(i)$ and $x(i + p)$ do not belong to an orbit of minimal period k, where k divides p. If p is a prime number there are only the period one orbits to search for. If p is not prime there are other orbits which can masquerade as a period p orbit. The decision is made by looking at the intermediate values $x(i + 1)$, $x(i + 2)$, etc., for repetitions.

A second subtlety is due to the existence of multiple orbits of a given periodicity. For example, there are 3 period 4 orbits in the logistic map for sufficiently large λ. Searching for the smallest distance $|x(i) - x(i + 4)|$ is a guarantee that we won't find more than one such orbit. As a useful rule of thumb, a first sweep is used to find the smallest difference, say 0.001. Then a threshold is set, say five times this smallest difference, and all values of $|x(i) - x(i + 4)|$ less than this threshold are located. Each difference will provide a quartet of x values: $x(i), x(i+1), x(i+2), x(i+3)$ as the coordinates in the orbit of period 4, together with $x(i + 4)$, which is compared with $x(i)$ to test goodness of the orbit. The x coordinates of all potential period four orbits are compared in the search for the three distinct period four orbits.

Once last piece of wisdom is useful. The search method above may find several different data segments representing the same orbit. The best should be used as the surrogate. However, it is not always useful to throw the others away. Comparing two or more surrogates of the same periodic orbit usually leads to important insights. For example, comparing two surrogates for a period one orbit in a flow reveals the local torsion in the flow around the period one orbit. This is an important characterization of part of the mechanism which generates chaotic behavior.

4.4   Phase Space Partitions

In many instances it is useful to be able to partition the phase space into a number of subregions which are non overlapping but contiguous. We have already used such decompositions for computing fractal dimensions. In the present case our aims will be different. First, we would like a small number of 'boxes,' the smaller the better. Second, we will use the decomposition to map dynamics in the phase space into a kind of symbolic dynamics. That is, each of the regions in the phase space will be assigned a symbol (*e.g.*, 0,1 or L, R for simple maps of the interval like the logistic map). Then each orbit in the phase space can be replaced by a string of symbols according to which box in the phase space is visited, and the order in which the boxes (or intervals) are visited.

4.4.1   Transition Graphs and Transition Matrices

In Fig. 4.3 we show a phase space which is part of the real line. It is divided into three subintervals (I, J, K). The return map is shown. This return map shows that the interval I is mapped *onto* the interval K. Similarly, K is mapped onto I, and J is mapped onto all three intervals. More mathematically, we could write $f(J) \supseteq I \cup J \cup K$. These relations are summarized on the right in a transition graph. The arrow from I to K says that $f(I)$ *covers* K, or that K is in the image of I (under f). Mathematically we write $f(I) \supseteq K$, and similarly for the arrow from K to I. Since the image of J covers everything, there are arrows from J to everybody. These relations are also very conveniently summarized in a (Markov) transition matrix. The rows and columns are labeled by the indices for the partition (*e.g.*, I, J, K). The matrix element $M_{ij} = 0$ if $f(I_i)$ does not cover I_j. If $f(I_i) \supseteq I_j$, $M_{ij} = 1$. The first row (I) of the 3×3 transition matrix for the return map of Fig. 4.3 is $(0, 0, 1)$. The entire matrix is

$$M = \begin{bmatrix} 0 & 0 & 1 \\ 1 & 1 & 1 \\ 1 & 0 & 0 \end{bmatrix} \tag{4.3}$$

Markov transition matrices are extremely useful for computing allowed and forbidden symbol sequences. They are also useful for computing topological entropy ($h_T = \log(\lambda_M)$, where λ_M is the largest eigenvalue of M).

Another example is given in Fig. 4.4. In this case the partition has four components. The return map is shown on the left and the transition graph is shown on the right. The Markov transition matrix is

$$M = \begin{bmatrix} 0 & 1 & 0 & 0 \\ 0 & 0 & 1 & 0 \\ 0 & 0 & 0 & 1 \\ 1 & 1 & 1 & 1 \end{bmatrix} \tag{4.4}$$

4.4.2   Fixed Point Theorem

There is an elegant theorem which tells us that if f is a smooth map of the connected set A and if $f(A) \supseteq A$, then there is at least one point in A which is invariant under the map. It is a *fixed point* of the map. The map shown in Fig. 4.3 has a fixed point in the interval J and the map shown in Fig. 4.4 has a fixed point in interval L. This theorem, the Brouwer fixed point theorem, is generally true (in n dimensional manifolds M^n), and not restricted to intervals in R^1.

4.4.3   Eigenvalues of M and Topological Entropy

It is a simple matter to check that the Markov transition matrix for the second iterate of f is the square of the Markov transition matrix M of f. More generally, the Markov matrix for $f^{(n)}$ is M^n. These matrices may have matrix elements

Figure 4.3: (Alligood., p. 128). The interval is partitioned into three contiguous segments. The return map is shown on the left. Its transition graph is shown on the right.
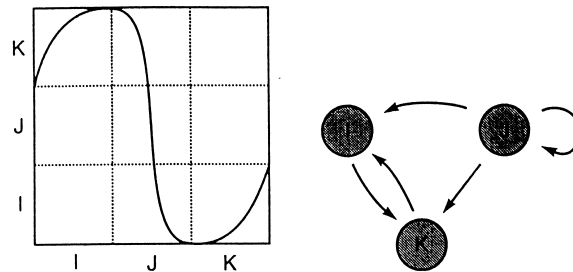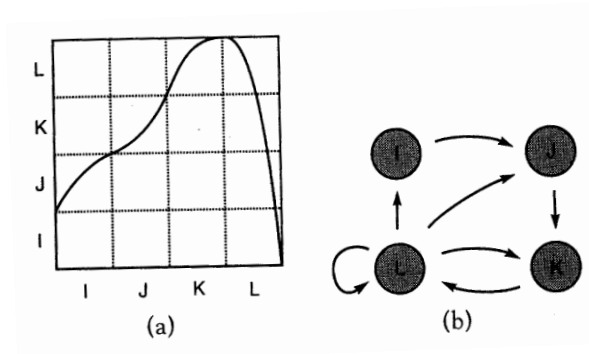

Figure 4.4: (Alligood., p. 129). The interval is partitioned into four contiguous segments. The return map is shown on the left. Its transition graph is shown on the right.

which are integers larger than one. For example, if $(M^4)_{ij} = 3$, there are 3 ways to get from i to j in 4 steps. If any matrix elements of the original Markov transition matrix M are larger than 1, a finer partition is necessary.

The Markov transition matrix can be used to estimate the number of fixed points of the nth iterate of a map. For example, the second and third iterates of the Markov transition matrix (4.4) for the map shown in Fig. 4.4 are

$$
M^2 = \begin{bmatrix} 0 & 0 & 1 & 0 \\ 0 & 0 & 0 & 1 \\ 1 & 1 & 1 & 1 \\ 1 & 2 & 2 & 2 \end{bmatrix}
\qquad
M^3 = \begin{bmatrix} 0 & 0 & 0 & 1 \\ 1 & 1 & 1 & 1 \\ 1 & 2 & 2 & 2 \\ 2 & 3 & 4 & 4 \end{bmatrix}
\qquad (4.5)
$$

The matrix M informs us that there is one fixed point of the original map f, and it is in the interval L. From M^2 we see that $f^{(2)}$ has one fixed point in K and two in L. The fixed point of $f^{(2)}$ in K corresponds to the orbit $K \to L \to K$. It is one point on an orbit of period 2. One of the two fixed points of $f^{(2)}$ in L is the fixed point of f in L (symbolic: LL). The other fixed point is the round trip $L \to K \to L$. This is the other point on the period two orbit.

The diagonal elements of the matrix M^3 can be analyzed similarly. We present the results in tabular form.

Matrix Element	Value	Trajectory	Orbit
$(M^2)_{KK}$	1	$K \to L \to K$	$(KL)_1$
$(M^2)_{LL}$	2	$L \to K \to L$	$(KL)_2$
		$L \to L \to L$	(L)
$(M^3)_{JJ}$	1	$J \to K \to L \to J$	$(JKL)_1$
$(M^3)_{KK}$	2	$K \to L \to J \to K$	$(JKL)_2$
		$K \to L \to L \to K$	$(KLL)_1$
$(M^3)_{LL}$	4	$L \to J \to K \to L$	$(JKL)_3$
		$L \to K \to L \to L$	$(KLL)_3$
		$L \to L \to K \to L$	$(KLL)_2$
		$L \to L \to L \to L$	(L)

$$(4.6)$$

These results tell us, for example, that there are four trajectories which begin in L and return to L in three steps. One belongs to the period one orbit (L), one is the third point on the period three orbit (JKL), and the remaining two are the second and third points on the period three orbit (KLL). There are three points on each of these period three orbits. For example, the three points on (JKL) have futures $JKL\,JKL\,J..$, $KLJ\,KLJ\,K..$, and $LJK\,LJK\,L...$ It is sufficient to identify only one point in the orbit in order to identify the entire orbit. We choose to identity each orbit using the point it its trajectory which is alphabetically earliest.

The number of fixed points of $f^{(n)}$ is the sum of the diagonal matrix elements of M^n, so that

$$
N(p) \sim \frac{1}{p}\,\mathrm{tr}\,M^p
$$

The trace of a matrix is invariant under a similarity transformation. In particular, if $\lambda_1 \geq \lambda_2 \geq \cdots$ are the eigenvalues of M, then

$$N(p) \sim \frac{1}{p} \sum_i \lambda_i^p$$

As p becomes large, the term which contributes most substantially to this sum is the largest eigenvalue λ_M. Therefore, $N(p) \sim \frac{1}{p}\lambda_M^p$, so that

$$h_T = \lim_{p \to \infty} \frac{\log(\lambda_M^p)}{p} = \lim_{p \to \infty} \left(\log(\lambda_M) - \frac{\log(p)}{p} \right) \to \log(\lambda_M) \qquad (4.7)$$

As a first application of this result, the largest eigenvalue of the Markov transition matrix (4.3) for the return map shown in Fig. 4.3 is $\lambda_M = 1$. The topological entropy for this map is $h_T = \log(1) = 0$. For the return map shown in Fig. 4.4, the Markov matrix is given in (4.4). For this matrix $\lambda_M = 1.927562$ and $h_T = 0.656256$. For the logistic map at $\lambda = 4$ the interval $[0, 1]$ has a simple partition into the left half L and the right half R. The Markov transition matrix is full: $\begin{bmatrix} 1 & 1 \\ 1 & 1 \end{bmatrix}$. It describes a full shift on two symbols. The eigenvalues are 2, 0. The topological entropy of the logistic map at $\lambda = 4$ is therefore $\log(2)$.

4.5 Bounds on Topological Entropy

It is a simple matter to establish bounds on the topological entropy of a return map. When the partition is 'clean,' as in the cases shown in Figs. 4.3 and 4.4, the topological entropy is the logarithm of the largest eigenvalue of the Markov matrix. A 'clean' partition is a partition in which the image of each subinterval (box) exactly covers a union of other subintervals:

$$f(I_i) = I_j \qquad \text{or} \qquad f(I_i) = \cup_j I_j$$

Exact partitioning is possible only in exceptional circumstances.

Instead, we introduce rules for constructing transition matrices which provide upper and lower bounds on the topological entropy. In both cases the interval (phase space) is divided into subintervals $I_1, I_2, \cdots$. The return map shown in Fig. 4.5 is used to illustrate these rules.

4.5.1 Rules L

The transition matrix elements are constructed as follows:

a. $M_{ij} = 0$ if $f(I_i) \cap I_j = \emptyset$.

b. $M_{ij} = 1$ if $f(I_i)$ *covers* I_j: $f(I_i) \supseteq I_j$

The transition matrix for the map in Fig. 4.5 constructed from these rules is

$$M_L = \begin{bmatrix} 0 & 0 & 1 \\ 1 & 1 & 1 \\ 1 & 0 & 0 \end{bmatrix} \tag{4.8}$$

These rules *under* estimate the number of periodic orbits. For example, these rules do not count the possibility that a symbol string contains the sequences ...AB... or ...CB..., which are allowed. The logarithm of the largest eigenvalue λ_L of M_L is a *lower* bound on the topological entropy.

4.5.2   Rules U

The transition matrix elements are constructed as follows:

a. $M_{ij} = 0$ if $f(I_i) \cap I_j = \emptyset$.

b. $M_{ij} = 1$ if $f(I_i)$ *intersects* I_j: $f(I_i) \cap I_j \neq \emptyset$

The transition matrix for the map in Fig. 4.5 constructed from these rules is

$$M_U = \begin{bmatrix} 0 & 1 & 1 \\ 1 & 1 & 1 \\ 1 & 1 & 0 \end{bmatrix} \tag{4.9}$$

These rules *over* estimate the number of periodic orbits. For example, these rules count the possibility that a symbol string contains the sequences ...ABC... or ...CBA..., which are forbidden. The logarithm of the largest eigenvalue λ_U of M_U is an *upper* bound on the topological entropy.

4.5.3   Limits as $\epsilon \to 0$

The idea is to partition phase space, construct transition matrices M_L and M_U according to the rules specified above, find the largest eigenvalues of these matrices, and use them as bounds on the topological entropy. For example, M_L in (4.8) above has largest eigenvalue $\lambda_L = 1$, while M_U in (4.9) above has largest eigenvalue $\lambda_U = 2.414213$. The bounds on h_T for this partition are

$$\log(1) = 0 \leq h_T \leq 0.881374 = \log(2.414213)$$

Then tearing a page from the folks who compute fractal dimensions, we repeat this construction for all possible partitions of the phase space as $\epsilon \to 0$. Here ϵ is the diameter of the largest box in the partition.

   This method will give convergent bounds for h_T in phase spaces of any dimension. However, it smacks too much of the aura of fractal dimension calculations, to say nothing of the impracticability of computing eigenvalues for very large matrices.
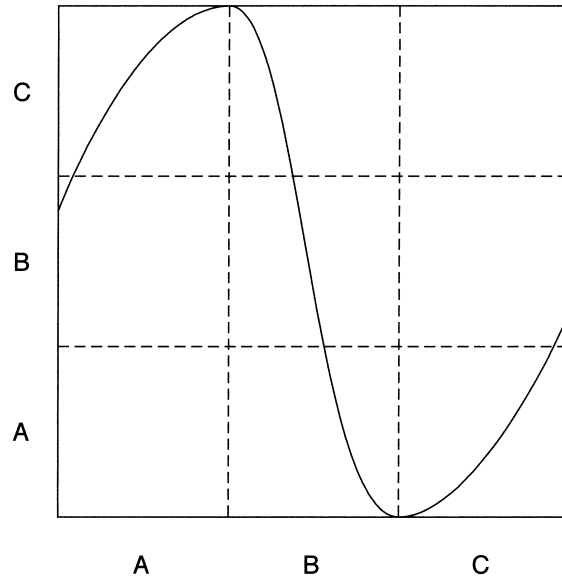
Figure 4.5: The partition shown here is not 'clean.' Markov transition matrices constructed according to the Rules L and U provide lower and upper bounds for this return map.

4.5.4 Alternatives

We reject this method for computing topological entropy. We will shortly see two (much) better methods for estimating h_T. One is based on computing the entropy for unstable (surrogate) orbits extracted from the chaotic attractor (Sec. 4.9). The other is based on the alphabet, words, and grammar of the symbol sequence representing a chaotic time series (Sec. 4.10).

4.6 Symbolic Coding and Dynamics

In this section we describe how to encode dynamics. That is, given a phase space and a dynamics which describes the evolution from initial conditions in the phase space, we will encode the trajectory with a symbol sequence.

4.6.1 Coding

A symbol sequence is determined by the order in which a trajectory visits boxes in a partition. As a simple example, consider the return map shown in Fig. 4.3

An initial condition in the subinterval I is forced to visit the subinterval K. After K, it is forced to return to I. This sequence repeats forever: $I \to K \to I \to ...$, more simply $IKIKI...$, and even more simply yet (IK). The ( ) indicates that whatever is within is repeated (forever). An initial condition in J can return to J as many times as it wants, until entering I or K, after which it bounces around between the two intervals as just described. Such an orbit has trajectory $J^n(IK)$ or $J^n(KI)$.

For the more interesting return map shown in Fig. 4.4 there are more possibilities. A number of these possibilities, up to period 3, have been shown in Eq (4.6). For example, two orbits of minimal period three were found: (JKL) and (KLL). We will often do away with the ( ) is representing periodic orbits.

Allowed symbol sequences can be constructed from the Markov transition matrix by extending their use in an intuitive way. We replace the symbol 1 everywhere it occurs in the row representing the interval I_i by the symbol I_i. Then take powers of this related matrix, treating the symbols as noncommuting operators. Two examples suffice. First, we make the transformation on the Markov matrix in (4.4):

$$\begin{bmatrix} 0 & 1 & 0 & 0 \\ 0 & 0 & 1 & 0 \\ 0 & 0 & 0 & 1 \\ 1 & 1 & 1 & 1 \end{bmatrix} \to \begin{bmatrix} 0 & I & 0 & 0 \\ 0 & 0 & J & 0 \\ 0 & 0 & 0 & K \\ L & L & L & L \end{bmatrix} \tag{4.10}$$

Now take the square of this new matrix:

$$\begin{bmatrix} 0 & I & 0 & 0 \\ 0 & 0 & J & 0 \\ 0 & 0 & 0 & K \\ L & L & L & L \end{bmatrix}^2 = \begin{bmatrix} 0 & 0 & IJ & 0 \\ 0 & 0 & 0 & JK \\ KL & KL & KL & KL \\ LL & LI+LL & LJ+LL & LK+LL \end{bmatrix} \tag{4.11}$$

The entry in the IK position is $(M^2)_{IK} = IJ$. This tells us there is one way to get from subinterval I to subinterval K in two steps, and this path takes us through subinterval J. The matrix element $(M^2)_{LL} = LK + LL$ tells us that there are two ways to return to L in two steps: the period one orbit $L (= (L))$ and the period two orbit KL.

The cube of this matrix gives information about how to move from any segment to any other in three steps. It is

$$M^3 = \begin{bmatrix} 0 & 0 & 0 & IJK \\ JKL & JKL & JKL & JKL \\ KLL & KLI+KLL & KLJ+LKL & KLK+KKL \\ LKL+ & LKL+LLI+ & LIJ+LKL+ & LJK+LKL+ \\ LLL & LLL & LLJ+LLL & LLK+LLL \end{bmatrix} \tag{4.12}$$

This matrix shows the seven fixed points of M^3 which were treated earlier. These paths can be visualized as allowed paths through the transition graph.

4.6.2 Dynamics

Each arrow in a transition graph represents a forward evolution by one time step. So does each entry 1 in the original Markov transition matrix M. Dynamics in the phase space can be represented by shifts in symbol space. For example, consider an initial condition in the interval J under the return map shown in Fig. 4.4. This point could iterate through the four subintervals according to $.JKLL\cdots$. Once the point passes through J it winds up in K. Its future from this interval is $.KLL\cdots$, and once it passes through K its future is $.LL\cdots$. As a result, we have the relation

Dynamics	Phase Space
Shifts	Symbol Space

4.6.3 Types of Orbits

Symbol sequences allow us to make simple and elegant distinctions between different types of orbits. There are essentially two types of orbits: periodic and chaotic. A periodic orbit of period p in phase space is one that repeats itself after p steps. In symbol space such an orbit is represented by a symbol sequence of length p which repeats itself forever. A chaotic orbit in phase space is one which is nonrepeating. It is represented in symbol space by a sequence of symbols which is nonrepeating.

It is possible to identify periodic orbits with rational fractions and chaotic orbits with irrational numbers. This can be done by assigning integer values to the elements of a partition. For example, we can assign the integers (0,1,2,3) to the subintervals (I, J, K, L) in Fig. 4.4. Then the two period three orbits (JKL) and (KLL) can be identified with the string of integers

$$
\begin{aligned}
(JKL) &\rightarrow (123) = 123\ 123\ 123\ ... \\
(KLL) &\rightarrow (233) = 233\ 233\ 233\ ...
\end{aligned}
$$

These infinite repeating sequences sum to rational fractions. We illustrate for the first of these orbits. The sequence 123 123 (etc.) is interpreted as a quaternary (since there are 4 subintervals in the original partition) representation of a real number, which is

$$
(123) \rightarrow \frac{1}{4} + \frac{2}{4^2} + \frac{3}{4^3} + \frac{1}{4^4} + \frac{2}{4^5} + \frac{3}{4^6} + \frac{1}{4^6} \times \left(\frac{1}{4} + \frac{2}{4^2} + \frac{3}{4^3}\right) + \cdots
$$

This sum can be carried out in closed form

$$
\left(\frac{1}{4} + \frac{2}{4^2} + \frac{3}{4^3}\right) \times \left(1 + \frac{1}{4^3} + \frac{1}{4^6} + \cdots\right) = \frac{1/4 + 2/4^2 + 3/4^3}{1 - \frac{1}{4^3}}
$$

This can be simplified even further by clearing fractions

$$
= \frac{1 \times 4^2 + 2 \times 4^1 + 3 \times 4^0}{4^3 - 1} = \frac{27}{63} \text{ base } 10
$$

The result is expressed more directly base 4:

$$\frac{123}{333}$$

This result is not accidental. The fraction identifying a period p orbit based on n symbols is the ratio of two numbers base n. The numerator is the symbol sequence for the identifying point in the orbit (alphabetically the earliest). The denominator is $n^p - 1$, whose symbol sequence consists of a string of p symbols n. With this insight, the rational fraction for (KLL) is swiftly determined

$$(KLL) \simeq (233) \rightarrow \frac{233}{333} \text{ base 4} = \frac{47}{63} \text{ base 10}$$

Chaotic orbits are represented by nonrepeating symbol sequences, which in turn translate into nonrepeating integer sequences, which in turn represent irrational numbers.

All rational fractions represent symbol sequences which are eventually periodic.

4.6.4   Metric in Symbol Space

The search for unstable periodic orbits in chaotic time series is simplified by introducing a metric in symbol space. The idea is to associate a pair of real numbers to each position in a symbol sequence. One real number describes the future from that point, the other describes the past. There is little real gain for data sets generated by one dimensional maps such as the logistic map: the data set $x(i)$ suffices in the search for periodic orbits. However, dynamics in 2-, 3-, n-dimensional phase spaces can often be reduced to symbol sequences. Once the dimension of the phase space is larger than one, a distinct reduction in computational overhead is realized by encoding the past and future of a symbol sequence by real numbers.

The procedure is suggested by the encoding of periodic orbits described above. Suppose we have a symbol sequence $...s_{i-2}\ s_{i-1}\ .\ s_i\ s_{i+1}\ s_{i+2}....$ based on an alphabet of n letters. The future from the ith symbol (the first behind the .) is represented by the real number

$$f_i = \frac{s_i}{n} + \frac{s_{i+1}}{n^2} + \frac{s_{i+2}}{n^3} + \frac{s_{i+3}}{n^4} + \frac{s_{i+4}}{n^5} + \cdots \tag{4.13}$$

More distant symbols are weighted less heavily than nearer symbols. Similarly, the past is represented by a real number in which the most recent events are weighted most heavily:

$$p_i = \frac{s_{i-1}}{n} + \frac{s_{i-2}}{n^2} + \frac{s_{i-3}}{n^3} + \frac{s_{i-3}}{n^4} + \frac{s_{i-3}}{n^5} + \cdots \tag{4.14}$$

Example: For the segment of chaotic data on an interval with four partitions (*c.f.*, Fig. 4.4) given by $\cdots 3321.2132 \cdots$ the future and past (measured from

the present, represented by .) are represented by real numbers with n-ary representations

$$\cdots 3321.2132\cdots \longrightarrow \quad \begin{aligned} f &= 2132\cdots \\ p &= 1233\cdots \end{aligned}$$

If the sequence is periodic, these n-ary representations can be written in closed form as rational fractions. For example, for the second point on the period three orbit (JKL), $\cdots 231\ 231.231\ 231\ 231\ \cdots$, we easily find

$$f = \frac{231}{333} = \frac{45}{63} \qquad p = \frac{132}{333} = \frac{30}{63}$$

The first fraction is base 4, the second base 10.

4.6.5   Initial Conditions and Coding

If you look at the shiny side of a CD, you will realize that everything on that side is a series of zeroes and ones. Everything is encoded in binary format.

   This means that there is some initial condition for the logistic map at $\lambda = 4$ which reproduces the symbol sequence of 0's and 1's on any CD.

   It is truly remarkable that some initial condition for the logistic map codes for BWV 232, another initial condition codes for Lear, yet another codes for Oedipus. Each of these symbol sequences is non periodic. That is, chaos can carry a great deal of aesthetic appeal.

   Remark: Many recordings exist of BWV 232, Lear, and Oedipus. All are recognizable (by us) as such, yet all different recordings are represented by different binary codes. This leads to the deep 'representability' problem: How many different codings exist for a given work?

4.6.6   Periodic Orbits and Rational Fractions

Every rational fraction describes an eventually repeating orbit, and vice versa. We illustrate this relation with an example. This example can be used as a model for a proof, if one is desired.

   First, we show that an eventually repeating orbit can be represented by a rational fraction. We take the trajectory $.22111\cdots = .2^2 1^\infty = .22(1)$ in the phase space illustrated in Fig. 4.4. The partition of the phase space into four parts allows us to encode every trajectory with four letters, variously I, J, K, L or $0, 1, 2, 3$. The rational fraction is obtained from

$$.221111\cdots \rightarrow \frac{2}{4} + \frac{2}{4^2} + \frac{1}{4^3} + \frac{1}{4^4} + \cdots = \frac{2\times 4^1 + 2\times 4^0}{4^2} + \frac{1}{4^2}\left(\frac{1}{4} + \frac{1}{4^2} + \cdots\right)$$

$$= \frac{22}{100} + \frac{1}{100}\times\frac{1}{3} = \frac{133}{300}$$

This fraction is base 4. Base 10, the fraction is $\frac{31}{48}$.

To construct a symbolic sequence from a rational fraction $f = \frac{31}{48}$, we proceed as follows (base 10). Construct an integer ($s_1 = 0, 1, 2, 3$) and a remainder fraction f_1 by

$$s_1 = [4 \times f] \qquad f_1 = 4 \times f - s_1$$

Repeat until recursion is reached.

f_{i-1}	$4 \times f_{i-1}$	s_i	f_i
31/48	31/12	2	7/12
7/12	7/3	2	1/3
1/3	4/3	1	1/3
1/3	4/3	1	1/3
$\vdots$	$\vdots$	$\vdots$	$\vdots$

The symbol sequence is read vertically down the third column: $\frac{31}{48} \to .221111 \cdots$. This can also be carried out base 4.

In general, a rational fraction describes a trajectory that settles to a periodic orbit after the initial transients die out. In this example, the transients last for two periods, and the ultimate periodic orbit is 1 and has period 1.

4.7   Addresses

Not only is it possible to identify periodic orbits and eventually periodic trajectories by rational fractions and chaotic orbits by irrational numbers. It is also possible to locate each point of the trajectory in phase space by a rational fraction (periodic or eventually periodic orbit) or an irrational number. The algorithm we are about to present allows us to construct the *relative* position of a point in a trajectory along the interval. In some instances we can construct the *exact* location of the point on the interval.

4.7.1   Parity

Consider two points, a and b, $a < b$ in the subinterval J in the partition shown in Fig. 4.4. Under the dynamical rules these two points are mapped into the subinterval K, and in addition $f(a) < f(b)$. When mapped again, they appear in subinterval L and $f^{(2)}(a) < f^{(2)}(b)$. However, when mapped again, their order is reversed: $f^{(3)}(a) > f^{(3)}(b)$. These third iterates may occur in the same subinterval (I, J, K, L) or in different subintervals. However they appear, their order along the line is reversed since they have been mapped through the *orientation reversing* subinterval L. If they are mapped a second time through L, their order will be reversed a second time (*i.e.*, restored).

We call the subintervals I, J, K orientation preserving, or *even parity* subintervals since the slope of the return map is positive in these subintervals. We call the subinterval L orientation reversing, or *odd parity*, since the slope of the return map is negative in this subinterval. Since endpoints and critical

points always bound subintervals, it is possible to assign a fixed parity to each subinterval of a partition.

4.7.2 Construction of Addresses

The algorithm for constructing addresses is as follows. The orientation preserving and reversing subintervals of the return map are identified. An order for the subintervals in a partition is established and the orientation preserving and reversing subintervals are identified. For the return map shown in Fig. 4.4 the order of the four subintervals is $I < J < K < L$, I, J, K are orientation preserving, and L is orientation reversing. Following passage through any orientation reversing subinterval, all the subsequent subintervals are reversed in order ($I \to L$, $J \to K$, $K \to J$, and $L \to I$). For example, for the symbol string $IJKLKLKLIJ...$ we perform the following operations:

$$IJKLKLKLIJ\cdots \to IJKL\bar{K}\bar{L}\bar{\bar{K}}\bar{\bar{L}}\bar{L}\bar{I}\bar{J}\cdots \qquad (4.15)$$

Another way to view this is as follows. From the viewpoint of any symbol in the trajectory, look to the past (the left), determine the parity of the symbol sequence preceeding the symbol, leave the symbol unchanged if the parity is even, or change the symbol (as above) of the parity is odd.

As an example, the symbol sequence for the point $.JKL\ JKL\ JKL\ \cdots$ is $.JKL\ \bar{J}\bar{K}\bar{L}\ \bar{\bar{J}}KL$.

The algorithm goes more smoothly if the letter symbols are replaced by integers: $0 \leftrightarrow I$, etc. Then the alphabetical order is replaced by integer order $0 < 1 < 2 < 3$, the first three are orientation preserving and the last is orientation reversing. Parity reversal is simply $i \to 3 - i$. The point $.123$ on the pereiod three orbit (123) has address

$$.123\ 123\ 123\ \cdots.123\overline{123}\overline{\overline{123}}\cdots = .123\ 210\ 123\ \cdots = (123\ 210)$$

In general, the address of a point in an orbit of period p has period p or $2p$, depending on whether the orbit is of even or odd parity, respectively.

As for orbits

a. The repeating sequence of length p or $2p$ is an n-ary representation for a rational fraction which can be summed explicitly. In the case above the sum is 123 210/333 333.

b. A metric can be placed on addresses. The future and past can be computed. For the example above, the future is 123 210/333 333 and the past is 012 321/333 333.

4.7.3 Periods 1, 2, 4, and 3

We take the usual partition $(0, 1)$ for the logistic map. The period one orbit (1) has address $1\bar{1}1\bar{1}1\cdots = (10)$. The addresses for the two points in the period 2

orbit (01) and the period four orbit (0111) of the period doubling cascade, and the two period three orbits (001) and (011) are constructed below.

Orbit	Point	Label	Construction	Address	Location
(01)	01		$01\ \bar{0}\bar{1}$	01 10	
	10		$1\bar{0}\ \bar{1}0$	11 00	
(0111)	0111	a	$01\bar{1}1\ \bar{0}\bar{1}1\bar{1}$	0101 1010	1
	1110	b	$1\bar{1}10\ \bar{1}1\bar{1}0$	1011 0100	3
	1101	c	$1\bar{1}01\ \bar{1}1\bar{0}\bar{1}$	1001 0110	2
	1011	d	$10\bar{1}1\ \bar{1}01\bar{1}$	1101 0010	4
(001)	001	α	$001\ \bar{0}\bar{0}\bar{1}$	001 110	1
	010	β	$01\bar{0}\ \bar{0}\bar{1}0$	011 100	2
	100	γ	$1\bar{0}0\ \bar{1}00$	111 000	3
(011)	011		$01\bar{1}\ 01\bar{1}$	010 010	
	110		$1\bar{1}0\ 1\bar{1}0$	100 100	
	101		$10\bar{1}\ 10\bar{1}$	110 110	

$$(4.16)$$

The three points α, β, γ on the period three orbit (001) are placed on the interval in accordance with their addresses in Fig. 4.6 (top). Under the dynamics, $\alpha \to \beta \to \gamma \to \alpha$. The four points a, b, c, d on (0111) are treated similarly in the lower part of Fig. 4.6. Under the dynamics $a \to b \to c \to d \to a$, but the order along the interval in which these points are visited is not preserved $(1 \to 3 \to 2 \to 4 \to 1)$.

A number of useful observations should be made.

1. All of the orbits participating in the period doubling cascade have odd parity.

2. The two period three orbits are created in a saddle node bifurcation. The even parity orbit is the saddle, the odd parity orbit is the node.

3. All odd parity orbits of period p have addresses of period $2p$. Even parity orbits of period p have addresses of period p.

4. The three points in the period three orbit (001) are labeled α, β, γ. Their relative locations are determined by their addresses. The relative positions of these three points on the interval are shown in Fig. 4.6 (top).

5. The four points in the period four orbit (0111) are labeled a, b, c, d. Their relative addresses show that their order along the interval is a, c, b, d. The relative positions of these four points on the interval are shown in Fig. 4.6 (bottom).

6. The address is a repeating infinite sequence. Only the basic unit, of period p or $2p$, is given for each address.
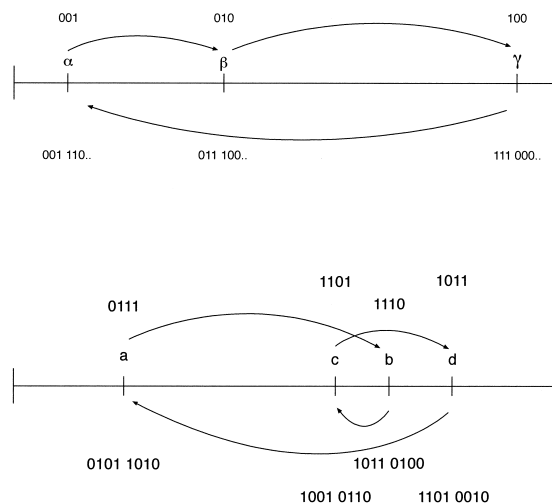
Figure 4.6: (top) The three points α, β, γ on the orbit (001) are placed on the interval according to their addresses, shown below the points. The map acts as shown by the arrows. (bottom) The same is shown for the four points a, b, c, d on the period four orbit (0111).

4.7.4 Rules on Order

The order in which points of periodic orbits appear on the interval constrains the order in which orbits are created by bifurcations when the control parameter of the logistic map is increased (or annihilated when λ is decreased).

This idea is illustrated in Fig. 4.7. Here the points on the period three orbit (001), the period four orbit (0111), and the period one (1) and two (01) are placed in order on the interval. Their order is determined by their addresses, determined in (4.16). The addresses do not determine the absolute location along the interval (except see below, Sec. 4.7.6), only the relative position.

In decreasing λ through the $2 \to 4$ bifurcation, the two points a and c join the leftmost point of the period 2 orbit in an inverse period doubling (cusp, A_3) bifurcation. Simultaneously, b and d join the rightmost point of (01). As λ decreases through first period doubling point, the two points on the period two orbit join the period one orbit in another bifurcation. This is shown in Fig. 4.7. If the period three orbit is still in existence in the control parameter range between the first and second period doubling bifurcation, then at some point the point β on (001) must intersect the trajectory of c, shown as a circle in Fig. 4.7. If it still exists in the range $2 \to 1$, then it will intersect the trajectory of one of the points of the period two orbit, also shown as a circle. This is not possible, since it violates a uniqueness theorem. This theorem says that

Figure 4.7: The locations of the points in the period three and four orbits are as given in Fig. 4.6. The locations of the period one orbit and the two points of the period two orbit are also indicated. If the period three orbit is still present during the inverse bifurcations $4 \to 2$ or $2 \to 1$, then forbidden forced intersections must occur (shown as circles). These violate a uniqueness theorem.

each point on the interval is the initial condition for a unique trajectory. The point β is on a period three orbit, c is on a period 4 orbit, 2 is on a period two orbit. As a result, the period three orbit (001) cannot be present in the control parameter interval between the first two period doublings. These arguments can be extended upward, to the $4 \to 8$, $8 \to 16$ (all the way to accumulation).

There are two useful ways to look at this:

a. As λ decreases, the period three orbit (001) must be annihilated in an inverse saddle node bifurcation with its partner saddle (011) before the period doubling cascade occurs.

b. As λ increases, the period doubling cascade must be completed before the period three orbits (001) and (011) can be created in a saddle node bifurcation.

The order in which points on saddle node partners are ordered on the interval provides strong restrictions on the order in which bifurcations can occur in one-dimensional maps as the control parameters are varied. This holds for mother-daughter orbits (*e.g.*, (01) $\to$ (0111)) as well.

We illustrate this point with two examples. The locations of the points on the period three (3_1) saddle node pair of orbits (011) and (001) are shown in Fig. 4.8

Table 4.2: Labels and addresses for saddle node paired points on the orbits 3_1, 4_2, and 5_3 are listed.

Orbit	Point	Address
3_1	001	001 110
	011	010
	010	011 100
	110	100
	100	111 000
	101	110
4_2	0001	0001 1110
	0011	0010
	0010	0011 1100
	0110	0100
	0100	0111 1000
	1100	1000
	1000	1111 0000
	1001	1110
5_3	00001	00001 11110
	00011	00010
	00010	00011 11100
	00110	00100
	00100	00111 11000
	01100	01000
	01000	01111 10000
	11000	10000
	10000	11111 00000
	10001	11110

(top). The pairs of points on the two orbits which become doubly degenerate at the saddle-node bifurcation are indicated. We have not provided the addresses to reduce clutter. The period four saddle node pair 4_2 is displayed similarly. The addresses and pairing of all points on these two orbits are provided in Table 4.2. Both pairs of orbits are present at the limit $\lambda = 4$. As λ is decreased, one pair must be annihilated before the other. The period four orbit pair must be destroyed before the period three pair because two linked period four orbit points fall between two linked period three orbit points. Proceeding in the other direction, the period three pair must be created before the period four pair as λ increases.

Similar systematics govern the bifurcation order of the saddle node pairs 4_2 ((0001), (0011)) and 5_3 ((00011),(00001)). The placement of these orbits on the interval is shown in Fig. 4.8 (bottom). The uniqueness argument requires that
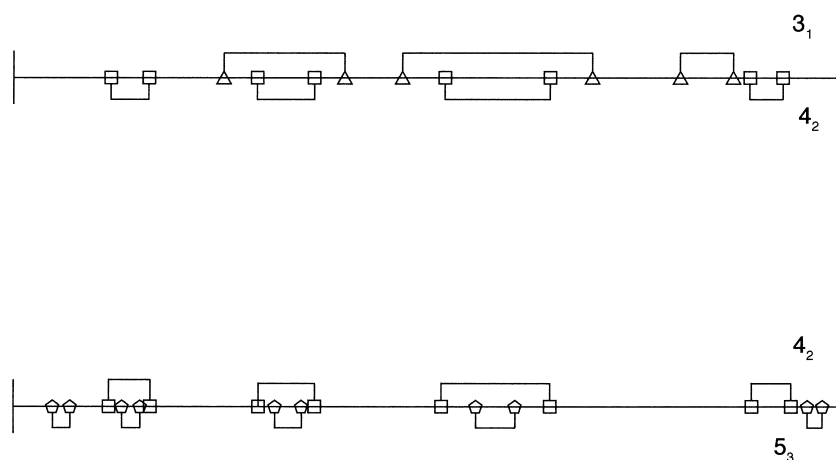
Figure 4.8: Pairs of points created together at saddle node bifurcations are linked. As λ decreases, inner pairs must be annihilated before outer pairs can be annihilated. (top) The orbit pair 4_2 must be annihilated before the orbit pair 3_1 can be annihilated. (bottom) The orbit pair 5_3 must be annihilated before the orbit pair 4_2 can be annihilated.

5_3 is annihilated before 4_2 (λ decreasing), or alternatively that 4_2 is created before 5_3 as a function of increasing λ.

Remark: The locations of points on the low period orbits can be determined by inspecting the bifurcation diagram. For higher period orbits, or low period orbits with narrow windows, this is difficult.

4.7.5   Bifurcation Order

The uniqueness theorem provides a method for determining the order in which orbits are created or annihilated in the logistic map. This order is rigid. For any two pairs of orbits (saddle-node pair or mother-daughter pair), the precedence can be determined by laying out the orbits on the interval and identifying corresponding (linking) pairs of points on orbits which become degenerate at the bifurcation. Then one linked pair will occur inside another linked pair. The inner linked pair belongs to the orbit pair which must first be annihilated before the other can be annihilated.

There is a somewhat simpler way to construct this universal bifurcation sequence. This will be described in the next Section.
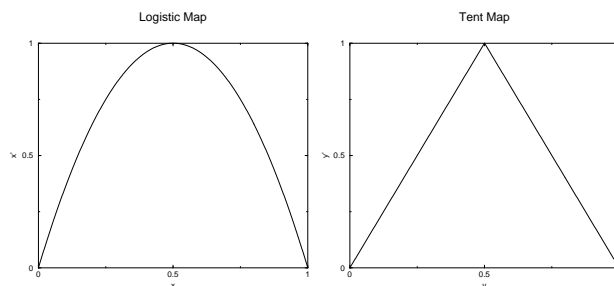
Figure 4.9: (left) Logistic map $x' = 4x(1 - x)$ and (right) tent map $y' = 2y$ for $0 \leq y \leq \frac{1}{2}$ and $y' = 2(1 - y)$ for $\frac{1}{2} \leq y \leq 1$ are both $2 \to 1$ maps of the unit interval onto itself.

4.7.6 Topological Conjugation

The addresses computed above (*c.f.*, Table 4.2) always provide the correct *order* for the iterates of the logistic map. They provide the exact location at the control parameter value $\lambda = 4$. In fact, they provide the exact location for the periodic orbits in a map which is related to the logistic map. This is the tent map:

$$y' = \begin{cases} \lambda' y & y \leq \frac{1}{2} \\ \lambda'(1 - y) & \frac{1}{2} \leq y \end{cases}$$

Both the logistic and tent maps are shown in Fig. 4.9. They both provide a $2 \to 1$ mapping of the unit interval onto itself at the extreme values $\lambda = 4$, $\lambda' = 2$. At $\lambda' = 2$, the addresses computed by the algorithm of Sec. 4.7.2 are exact locations (in binary code) for points on an orbit under tent map dynamics.

A simple smooth transformation exists for mapping between the logistic map and the tent map at these control parameter values. These maps are therefore *topologically conjugate*. The mapping is

$$x = \frac{1}{2}(1 - \cos(\pi y))$$

This curve is plotted in Fig. 4.10.

In order to find the exact location on the unit interval of a point on a trajectory under the logistic map ($\lambda = 4$), compute its address as described in Sec. 4.7.2. This address is the exact location of the point on the corresonding orbit under the tent map ($\lambda' = 2$). The address is the binary representation of the point (under Eq. (4.13)). Take this y value for the tent map coordinate, and convert it to the x value for the logistic map coordinate, using the transformation above.
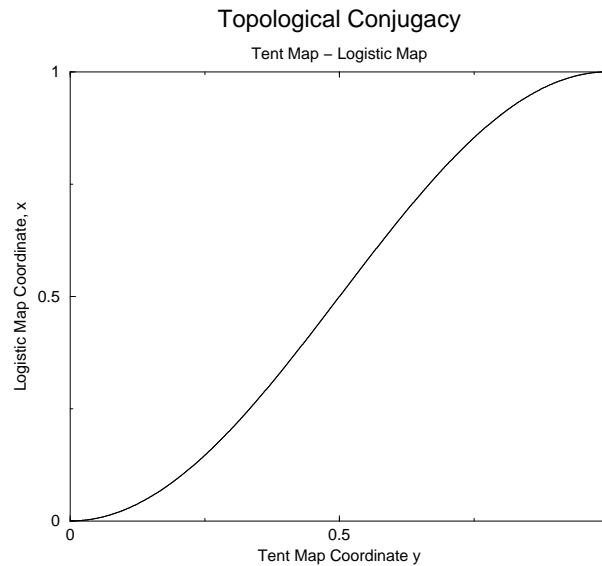
Figure 4.10: The smooth function $x = \frac{1}{2}(1 - \cos(\pi y))$ maps the tent map coordinate y to the logistic map coordinate x.

4.8   Universal Sequence

Topological arguments combined with the uniqueness theorem require orbits to be created in a particular order as a function of increasing control parameter for the logistic map. The topological arguments involve the existence of paired points in saddle-node pairs of orbits which become degenerate at the saddle-node bifurcation, and the presence of one set of paired points between another. The uniqueness theorem forbids a single point to be an initial condition for two inequivalent orbits. It is possible, but not practical, to build up the unique order in which orbits are created using these arguments. A simpler way is available.

4.8.1   Creation at the Top

Fig. 4.11 illustrates what happens when the period three orbit pair 3_1 is created in a saddle-node bifurcation. Just before the third iterate $f^{(3)}(x)$ becomes tangent to the diagonal at three points, the period three orbit pair does not exist but makes its presence known through the phenomenon of intermittency. At the triple tangency, each of the three tangent points describes a doubly degenerate point on an orbit. In fact, the saddle and node are degenerate at tangency. One degenerate pair of points is in the left hand interval and a second is in the right hand interval. However, the third pair of points is almost exactly at the maximum of the map. At the three tangent points, the slope of $f^{(3)}(x)$ is $+1$. Slightly after the tangency, the three points are nondegenerate but remain
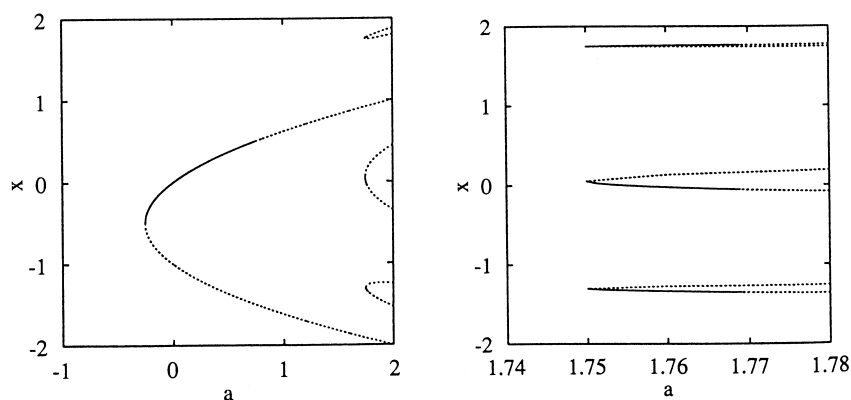
Figure 4.11: (Alligood p. 454) After the saddle node bifurcation creating the period three orbit pair, one of the doubly degenerate points created near the critical point moves to the right, the other moves to the left.

close. The pair in the left half remain on the left, and similarly for the pair on the right. In the middle, the right most point moves further to the right. The slope of $f^{(3)}(x)$ remains greater than one. This point belongs to the saddle orbit. Its partner moves to the left. As it does, its slope decreases from $+1$. When this point reaches the critical point $x = C$, the slope of $f^{(3)}(x)$ becomes zero. The Lyapunov exponent of this orbit becomes $-\infty$. The orbit is superstable. As λ continues to increase, the slope continues to decrease, eventually reaching -1, where the first period doubling bifurcation from this node occurs. The region in which the period three node is stable is shown by solid curves in Fig. 4.11.

All saddle node orbit pairs behave the same way when created. This behavior allows us to determine the order in which orbits are created in the logistic map as the control parameter λ increases. We use the critical point C ($x = \frac{1}{2}$ in the logistic map) as the initial condition for an orbit, iterate p times, and determine the values of λ at which the pth iterate returns to C. In fact, a plot of $f^{(p)}(\frac{1}{2}) - \frac{1}{2}$ (for the logistic map) as a function of λ will reveal all the control parameter values at which period p nodes become superstable.

These control parameter values are given in Table 4.3 for all orbits to period 7 in the logistic and sine maps. This table also provides the period and symbolic name of the orbit. The symbol name consists of $p - 1$ symbols. The pth symbol is assumed to be C. Here is how to read this table. There are three period 5 orbits. They are

$$C \to R \to L \to R \to R \to C$$
$$C \to R \to L \to L \to R \to C$$
$$C \to R \to L \to L \to L \to C$$

Each of these symbol sequences represents both a saddle and a node. The
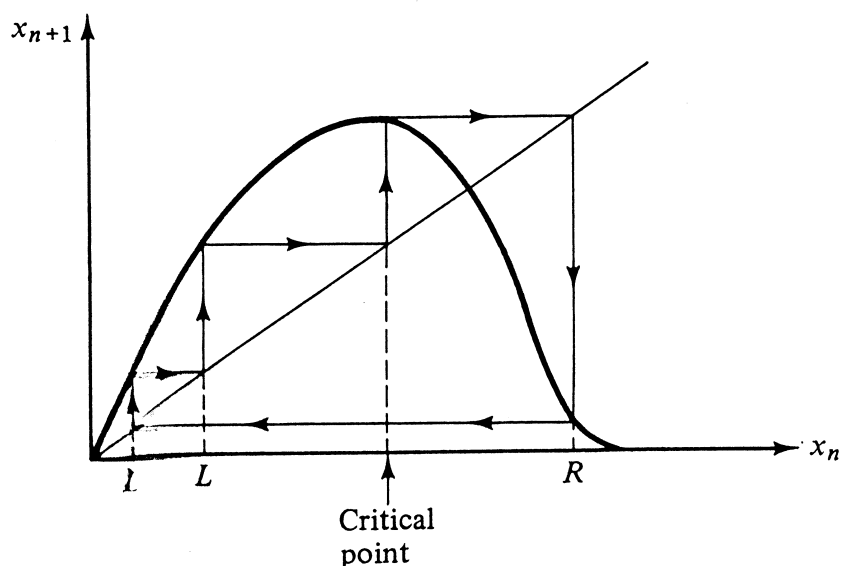
Figure 4.12: (Ott p. 50) At creation by saddle node bifurcation, one pair of degenerate points is created in the neighborhood of the critical point C. Its image is the furthest point on the right of the map. Its second image is the furthest point on the left of the map. The orbit shown is the period four orbit 4_2 with trajectory $(C)RLL$.

symbol sequences are obtained by replacing the first symbol C by L and R. For example, for the first period 5 orbit

$$CRLRR \longrightarrow \begin{array}{ll} LRLRR & \text{node} \\ RRLRR & \text{saddle} \end{array}$$

The saddle and node are distinguished by their parity: the saddle has even parity, the node has odd parity ($\mathcal{P}(L) = 0$, $\mathcal{P}(R) = 1$). The trajectory for the saddle node pair 4_2 ($CRLL$) at creation is shown in Fig. 4.12.

Members of period doubling cascades can similarly be distinguished. All are nodes, so all must have odd parity. The first two orbits in Table 4.3, of period 2 and 4, have symbolics $CR \rightarrow LR$ and $CRLR \rightarrow RRLR$ by parity arguments. The period three node has symbol sequence $CRL \rightarrow LRL$ and its period double has symbol name $CRLLRL \rightarrow RRLLRL$ by parity arguments.

4.8.2   Relation Between L, R and $0, 1$ Labels

Two related ways exist to label orbits in the logistic map. These are the L, R symbolics, used above to describe the U-Sequence, and the 0,1 symbolics, used

Table 4.3: Twenty one orbits are tabulated in their order of occurrence in both the logistic map $x' = \lambda x(1 - x)$ and the sine map $x' = q\sin(\pi x)$.

P_j	Symbol	λ	q
2_1	R	3.2360680	0.7777338
4_1	RLR	3.4985617	0.8463822
6_1	RLR^3	3.6275575	0.8811406
7_1	RLR^4	3.7017692	0.9004906
5_1	RLR^2	3.7389149	0.9109230
7_2	RLR^2LR	3.7742142	0.9213346
3_1	RL	3.8318741	0.9390431
6_2	RL^2RL	3.8445688	0.9435875
7_3	RL^2RLR	3.8860459	0.9568445
5_2	RL^2R	3.9057065	0.9633656
7_4	RL^2R^3	3.9221934	0.9687826
6_3	RL^2R^2	3.9375364	0.9735656
7_5	RL^2R^2L	3.9510322	0.9782512
4_2	RL^2	3.9602701	0.9820353
7_6	RL^3RL	3.9689769	0.9857811
6_4	RL^3R	3.9777664	0.9892002
7_7	RL^3R^2	3.9847476	0.9919145
5_3	RL^3	3.9902670	0.9944717
7_8	RL^4R	3.9945378	0.9966609
6_5	RL^4	3.9975831	0.9982647
7_9	RL^5	3.9993971	0.9994507

generally to describe experimental data. They are closely related. In the L, R classification, the first point on the orbit is closest to the critical point C. Therefore, the next point on the orbit is furthest to the right, and the point after is furthest to the left on the interval. Since the first point C is generally not given in the symbol name, the L, R symbolics starts with R, and the second symbol is L. These two points are, respectively, the point the furthest to the right and the point furthest to the left in the orbit. All other points in the orbit are between these two points.

In symbol sequences based on the symbols 0,1, it is customary to identify an orbit 'alphabetically.' This means the orbit is identified by the point which is furthest to the left on the interval. This corresponds to the first L in the L, R symbol name. The relation between these two ways of representing orbits involves a cyclic permutation and the relation $L \leftrightarrow 0$, $R \leftrightarrow 1$.

Example: The second period five orbit in Table 4.3 is identified as $RLLR = (C)RLLR$. We unwind this to alphabetic order $(C)RLLR \rightarrow LLRCR$ and then replace L by 0 and R by 1 to obtain 001$\underline{1}$1. The $\underline{1}$ means that the symbol underlined may be 0 or 1 for the saddle or node. As usual, which is which is determined by parity. The saddle is 00101 and the node is 00111. For nodes in a period doubling cascade the relation is similar. For example, for the first period four orbit in Table 4.3, we have $RLR = (C)RLR \rightarrow LRCR$. The critical point C must be replaced by L or R so the parity is that of a node: odd. The $0, 1$ symbol name is therefore 0111.

4.8.3   Saddle-Node Pairs

In the $0, 1$ notation, saddle node pairs of orbits are represented by symbol strings beginning with a 0, ending with a 1, whose penultimate (next to last) symbol is 0 or 1, depending on whether the orbit is a saddle or node. For example, the third period five orbit has symbol name 000$\underline{1}$1. This describes both the saddle 00011 and the node 00001.

4.8.4   Period-Doubling Systematics

Symbol names for nodes belonging to a period doubling cascade are built up easily and systematically by the following algorithm, which is illustrated for the cascade based on the period three node 001. The node symbol sequence of length p is repeated (this produces an even parity word of length $2p$) and the penultimate symbol is changed. This step is repeated forever.

$$001 \rightarrow 001\ 0\underline{0}1 = 001\ 011 \rightarrow 001\ 011\ \ 001\ 0\underline{1}1 = 001\ 011\ \ 001\ 001 \rightarrow \cdots$$

4.8.5   An Aufbau Algorithm

The control parameter values at which nodes become superstable can be determined by solving the equation $f^{(p)}(\frac{1}{2}) - \frac{1}{2} = 0$ (for the logistic map). This allows us to construct an order for creation of orbits of period p, for $p = 2, 3, \cdots$. The order in which orbits up to period 7 are created is presented in Table 4.3.

There is a general method available to list orbits in their order of creation. For each orbit, determine the address of the leftmost (or rightmost) point in the orbit. Then the order in which orbits are created is monotonic in these addresses. The further left the leftmost address (right for the rightmost), the later the orbit is created.

This observation has been implemented in a relatively simple algorithm for extending the ordered list of orbits. The algorithm is given in the L, R representation. Suppose we have a list of orbits up to period K by their order of creation in a unimodal map of the interval. This list can be extended to period $K+1$ as follows. Take two successive entries in this list, W_1 and W_2 of periods k_1 and k_2. Then higher period orbits will occur between these two. This algorithm determines which, their period, and their symbolics. Construct the harmonic extension of W_1 and the antiharmonic extension of W_2. These extensions are defined as follows:

$$
\begin{aligned}
H(W_1) &= W_1 \mu W_1 \\
A(W_2) &= W_2 \mu W_2
\end{aligned}
$$

The value of the symbol μ (L or R) depends on the parity of the symbol according to

Parity of W	+	−
Extension		
Harmonic	R	L
Antiharmonic	L	R

These two extensions will have $k^* > K$ of their leading symbols in common. If $k^* \geq 2k_1$ symbols are in common, they represent the period doubled orbit of W_1. If $k^* < 2k_1$ they represent an orbit of period $k^* + 1$ which is intermediate between W_1 and W_2.

We illustrate by extending the ordered list of orbits in the logistic map from period 4 to period 5. Up to period 4, the list of orbits is

P_j	W	$H(W)$	$A(W)$
2_1	R	RLR	
4_1	RLR	$RLRRRLR$	$RLRLRLR$
3_1	RL	$RLLRL$	$RLRRL$
4_2	RLL		$RLLRRLL$

From the results above, we see that $H(4_1) \cap A(3_1) = RLRR = 5_1$ and $H(3_1) \cap A(4_2) = RLLR = 5_2$. The last period five orbit $5_3 = RLLL$ can be appended to this list, which now grows to

P_j	W	$H(W)$	$A(W)$
2_1	R	RLR	
4_1	RLR	$RLRRRLR$	$RLRLRLR$
5_1	$RLRR$	$RLRRLRLRR$	$RLRRRRLRR$
3_1	RL	$RLLRL$	$RLRRL$
5_2	$RLLR$	$RLLRRRLLR$	$RLLRLRLLR$
4_2	RLL	$RLLLRLL$	$RLLRRLL$
5_3	$RLLL$		$RLLLRRLLR$

From this extended list we see $H(4_1) \cap A(5_1) = RLRRR = 6_1$. The antiharmonic of 3_1 must be extended beyond 5 letters. It is $A(3_1) = (RLRRL)R(RLRRL)$. Then $H(5_1) \cap A(3_1) = RLRRLR$, which describes a period 7 orbit. We also have $H(3_1) = (RLLRL)R(RLLRL) \cap A(5_2) = RLLRLR = 6_2$. This orbit is the period doubled orbit of the node in 3_1. We also find $H(5_2) \cap A(4_2) = RLLRR = 6_3$ and $H(4_2) \cap A(5_3) = RLLLR = 6_4$. Finally, we append the last period six orbit pair $6_5 = RLLLL$. For period six, there are four saddle node pairs together with one period doubled orbit of a period three, giving a total of nine distinct period six orbits.

The list of orbits in the U-Sequence, up to period 11, is given in the Appendix to this Chapter.

4.9 Topological Entropy of Orbits

The topological entropy of a return map can be computed by partitioning the phase space, computing Markov type transition matrices according to the Rules L and U for lower and upper bounds, computing the largest eigenvalue for these matrices, and taking logarithms. There are two simpler ways to estimate the topological entropy of a map. One depends on the properties of periodic orbits associated with the map. This method will be described in the present Section. The second method relies on the properties of the symbol string representing a chaotic trajectory. It will be described in the following Section.

4.9.1   Permutations

A permutation group operation can be assigned to every periodic orbit. The algorithm is simple. The points in an orbit can be described in two ways: by their symbolic code, and by the symbolic code of their addresses. The permutation assigned to an orbit is the group element which maps one assignment into the other.

We give meaning to the incantation above by carrying out an example. We compute the permutation for the orbit 0111, the period four orbit in the initial period doubling cascade. Listed below is the order in which the points in the orbit are visited and their addresses:

Label	Point	Address	Label
a	0111	0101 1010	1
b	1110	1010 0101	3
c	1101	1001 0110	2
d	1011	1101 0010	4

The order of these four points along the interval is shown in Fig. 4.6. The order in which the points are visited is $a \to b \to c \to d$. The four points are labeled $(1, 2, 3, 4)$ in order of their occurrence in the interval. The dynamical order (a, b, c, d) is not usually the same as their geometric order $(1, 2, 3, 4)$. Fig. 4.6 shows that when $a \to b$, the transition is from the first point in the interval

to the third. In the same way, $b \to c \sim 3 \to 2$, $c \to d \sim 2 \to 4$, and for closure, $d \to a \sim 4 \to 1$. We can thus associate the permutation (1324) with the orbit (0111). Every orbit can be assigned a permutation in this way.

4.9.2 'Clean' Partitions
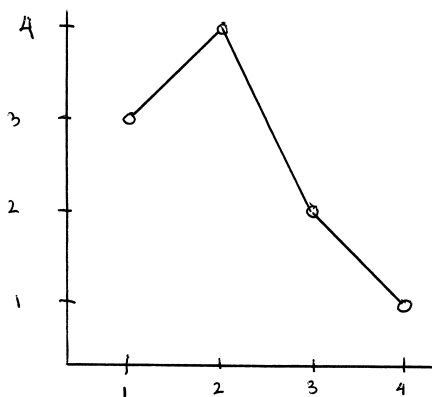
Figure 4.13: The four points in the orbit of (0111) provide a 'clean' partition of the interval into three subintervals. The return map on these subintervals is shown. This map is used to construct a transition matrix, from which the topological entropy is computed.

The points in a periodic orbit provide good points for a partition of the interval into subintervals. This partition can be used to estimate the topological entropy for that periodic orbit. This is an estimate of the number of periodic orbits (by period) which the existence of the original periodic orbit implies (forces). We illustrate the idea first for the period four orbit (0111) whose permutation is (1324). The construction is illustrated in Fig. 4.13. The four points on this orbit are used to partition the interval between the extremal points 1 and 4 into three subintervals I_{12}, I_{23}, and I_{34}. Then a return map is drawn. This shows that 1 is mapped to 3, 2 to 4, 3 to 2, and 4 to 1. Since $f(1) = 3$ and $f(2) = 4$, $f(I_{12}) = I_{34}$. We also easily see that $f(I_{23}) = I_{23} \cup I_{34}$ and $f(I_{34}) = I_{12}$. From this, or directly by inspection of the return map for the partition using this orbit, we find the following Markov transition matrix

$$\begin{bmatrix} 0 & 0 & 1 \\ 0 & 1 & 1 \\ 1 & 0 & 0 \end{bmatrix}$$

The largest eigenvalue of this matrix is $+1$, so the topological entropy of this orbit is 0. This makes sense, since this period four orbit does not imply the

existence of anything but its mother period two orbit (01) and its grandmother (1).
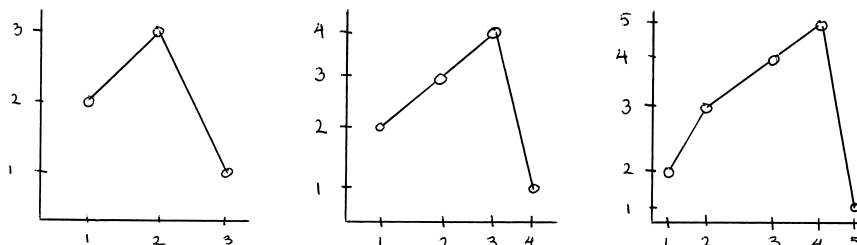
Figure 4.14: Three, four, and five points on the orbits 3_1, 4_2, and 5_3 divide the interval into two, three, and four subintervals (left to right). The return maps for these 'clean' partitions are shown.

Three more interesting cases are shown in Fig. 4.14. These are the return maps for the three orbits 3_1, 4_2, and 5_3. For these three orbits we have

$$
\begin{array}{cccc}
\text{Orbit} & 3_1 & 4_2 & 5_3 \\
\text{Permutation} & (123) & (1234) & (12345) \\
\\
\\
\text{Transition} & \begin{bmatrix} 0 & 1 \\ 1 & 1 \end{bmatrix} & \begin{bmatrix} 0 & 1 & 0 \\ 0 & 0 & 1 \\ 1 & 1 & 1 \end{bmatrix} & \begin{bmatrix} 0 & 1 & 0 & 0 \\ 0 & 0 & 1 & 0 \\ 0 & 0 & 0 & 1 \\ 1 & 1 & 1 & 1 \end{bmatrix} \\
\text{Matrix} & & & \\
\\
\\
\lambda & 1.618033989 & 1.839286755 & 1.927561975 \\
h_T & 0.481211825 & 0.609377863 & 0.656255979
\end{array}
\tag{4.17}
$$

4.9.3 Table of Values

The topological entropy is given for the orbits in the U-Sequence, up to period 8, in Table 4.4. This table provides the order of occurrence within the set of orbits of the same period, P_j, the symbolic name, the permutation, and the topological entropy. It also provides some additional information about these orbits, some of which will be used later.

4.9.4 Last Period p Orbit

The topological entropy of the last period p orbit created approaches $\log 2$ as $p \to \infty$. It is possible to find a scaling relation for the entropy in this limit. The last period p orbit has a cyclic permutation $(1, 2, 3, \cdots, p-1, p)$. Its topological entropy is constructed from a $(p-1) \times (p-1)$ matrix whose structure is easily

Table 4.4: Orbits up to period eight in the logistic map are shown in the order of their creation. Also shown is the symbol name of the orbit, the permutation of points along the interval, and its topological entropy.

P_j	Symbol	Permutation	Remark	Fraction	h_T
2_1	01	12	PD of 1		0.000000
3_1	0$\underline{1}$1	123	WO	1/3	0.481212
4_1	0111	1324	PD of 01		0.000000
4_2	00$\underline{1}$1	1234	WO	1/4	0.609378
5_1	011$\underline{1}$1	13425	WO	2/5	0.414013
5_2	001$\underline{1}$1	12435	QOD	1/3	0.543535
5_3	000$\underline{1}$1	12345	WO	1/5	0.656256
6_1	0111$\underline{1}$1	143526	FO		0.240606
6_2	001011	135246	PD of 3_1		0.481212
6_3	0011$\underline{1}$1	124536	FO		0.583557
6_4	0011$\underline{1}$1	123546	QOD	1/4	0.632974
6_5	000$\underline{1}$1	123456	WO	1/6	0.675975
7_1	01111$\underline{1}$1	1453627	WO	3/7	0.382245
7_2	0110$\underline{1}$1	1462537	QOD	2/5	0.442138
7_3	0010$\underline{1}$1	1362547	PE		0.522315
7_4	00111$\underline{1}$1	1254637	PE		0.562400
7_5	00110$\underline{1}$1	1356247	WO	2/7	0.601001
7_6	0001$\underline{0}$1	1246357	PE		0.618362
7_7	00011$\underline{1}$1	1235647	PE		0.645710
7_8	00001$\underline{1}$1	1234657	QOD	1/5	0.666215
7_9	00000$\underline{1}$1	1234567	WO	1/7	0.684905
8_1	01110101	15472638	PD of 4_1		0.000000
8_2	011111$\underline{1}$1	15463728	FO		0.304688
8_3	01101$\underline{1}$1	14725638	WO	3/8	0.468258
8_4	00101$\underline{1}$1	13725748	PE		0.499747
8_5	00101$\underline{0}$1	13647258	PE		0.539792
8_6	00111$\underline{0}$1	13657248	PE		0.547612
8_7	00111$\underline{1}$1	12564738	PE		0.574865
8_8	00110$\underline{1}$1	12573648	PE		0.591718
8_9	00010011	13572468	PD of 4_2		0.609378
8_{10}	00010$\underline{1}$1	12473658	PE		0.626443
8_{11}	00011$\underline{1}$1	12365748	PE		0.639190
8_{12}	00011$\underline{0}$1	12467358	FO		0.651766
8_{13}	00001$\underline{0}$1	12357468	PE		0.660791
8_{14}	00001$\underline{1}$1	12346758	PE		0.671317
8_{15}	00000$\underline{1}$1	12345768	QOD	1/6	0.680477
8_{16}	00000$\underline{0}$1	12345678	WO	1/8	0.689121

determined by inspection of 4.17. The secular equation obeys a simple recursion

$$S_p = \det \begin{bmatrix} -x & 1 & & & & \\ & -x & 1 & & & \\ & & -x & & & \\ & & & & -x & 1 \\ 1 & 1 & 1 & & 1 & 1-x \end{bmatrix} = (-x)S_{p-1} + (-1)^p$$

This recursion is initialized with $S_1 = 1$, so that $S_2 = 1 - x$ and $S_3 = (-x)(1 - x) - 1 = x^2 - x - 1$. The following snippet of Maple code computes the topological entropy for the last period p orbit:

```
s[1] := 1 : d[1] := 0.5 :
for p from 2 to 21 do
s[p] := (-x) * s[p - 1] + (-1)^p :
d[p] := fsolve(s[p], x = d[p - 1]..2) :
print(p, d[p], log(d[p]), log(2.0) - log(d[p])) : od :
```

These results are shown in Table 4.5. It is clear that the largest eigenvalue approaches 2 and the topological entropy approaches $\log(2)$ as $p \to \infty$.

We now construct a scaling relation. The largest eigenvalue of $S_p(x)$ is $2 - \epsilon_p$, with ϵ_p small. The recursion can be written

$$S_p(2 - \epsilon_p) = -(2 - \epsilon_p)S_{p-1}(2 - \epsilon_p) + (-1)^p$$

Taylor expanding and simplifying yields

$$\epsilon_p = \frac{2S_{p-1}(2) + (-1)^p}{S_{p-1}(2) + 2S'_{p-1}(2)}$$

The value and slope of the secular equation at $x = 2$ obey recursion relations, as follows:

p	$S_p(2))$	$S'_p(2)$
2	-1	-1
3	$+1$	$+3$
4	-1	-7
5	$+1$	$+15$
p	$(-1)^{p-1}$	$(-1)^{p-1}(2^{p-1} - 1)$

As a result, $\epsilon_p = 1/(2^{p-1} - 1)$, $\lambda_p = 2 - 1/(2^{p-1} - 1)$, $h_T \simeq \log(2 - 1/(2^{p-1} - 1)) \simeq \log(2) - \frac{1}{2}\frac{1}{2^{p-1}-1}$. The topological entropy of P_ω approaches $\log(2)$ like $\log(2) - \frac{1}{2^p}$.

4.9.5   First Odd Period Orbits

??? To be supplied ??? (Maybe)

Table 4.5: The topological entropy of the last orbit of period p approaches $\log(2)$ geometrically. This table provides the maximum eigenvalue of the characteristic equation for the transition matrix, its logarithm, which is the topological entropy h_T of the orbit, and the difference between $\log(2)$ and h_H.

Period	λ_{Max}	h_T	$\log(2) - h_T$
2	1.000000000	0.000000000	0.6931471806
3	1.618033989	0.4812118252	0.2119353554
4	1.839286755	0.6093778633	0.0837693173
5	1.927561975	0.6562559790	0.0368912016
6	1.965948237	0.6759746923	0.0171724883
7	1.983582843	0.6849047262	0.0082424544
8	1.991964197	0.6891211856	0.0040259950
9	1.996031180	0.6911607990	0.0019863816
10	1.998029470	0.6921614299	0.0009857507
11	1.999018633	0.6926563766	0.0004908040
12	1.999510402	0.6929023516	0.0002448290
13	1.999755501	0.6930249236	0.0001222570
14	1.999877833	0.6930860952	0.0000610854
15	1.999938939	0.6931166496	0.0000305310
16	1.999969475	0.6931319179	0.0000152627
17	1.999984739	0.6931395500	$0.76306 \, 10^{-5}$
18	1.999992370	0.6931433656	$0.38150 \, 10^{-5}$
19	1.999996185	0.6931452731	$0.19075 \, 10^{-5}$
20	1.999998093	0.6931462271	$0.9535 \, 10^{-6}$

4.10 Topological Entropy from Symbolic Dynamics

The problem of computing the topological entropy of a dynamical system is isomorphic to the problem of computing the capacity of a transmission channel. This problem was solved many years ago. The review that follows is a slightly paraphrased version of the summary in the first three pages of Shannon's classic paper (BSTJ, 1948).

4.10.1 Alphabet, Words, Grammar

Chaos has a lot in common with human communication. Explicitly, we use an alphabet to create words, and words to create messages. In nonlinear dynamics an alphabet consists of the basic symbols which we use to construct an orbit. In many cases we can collect subsets of symbols (*e.g.*, 01, 011, 0111) which appear very frequenty in a 'message.' The message is the symbol name for a chaotic orbit. These subsets are called 'words' for an obvious reason. Once we have words, a grammar follows. Rules of grammar tell us that some words naturally follow others; other word sequences may be forbidden. In chaotic dynamics, it often happens that there is a small vocabulary of words, and that the rules of the grammar allow any word to be followed by any other word.

4.10.2 Results of Finite Difference Theory

The capacity of a transmission channel is

$$C = \lim_{T \to \infty} \frac{1}{T} \log\ N(T)$$

Here $N(T)$ is the number of allowed signals of duration T, and log is to base e.

First, assume that a grammar contains n symbols $S_1, S_2, \cdots, S_n$ of lengths $t_1, t_2, \cdots, t_n$, and that every possible symbol sequence is allowed. The number of symbol sequences of length t is

$$N(t) = N(t - t_1) + N(t - t_2) + \cdots + N(t - t_n)$$

A well known result from the theory of finite difference equations states that $N(t)$ is asymptotic to AX_0^t, where A is a constant and X_0 is the largest real solution of the characteristic equation

$$X^t = X^{t-t_1} + X^{t-t_2} + \cdots + X^{t-t_n}$$

or equivalently

$$1 = X^{-t_1} + X^{-t_2} + \cdots + X^{-t_n} \tag{4.18}$$

As a result, $C = \log X_0$.

In many grammars, not all symbol sequences are allowed (qu is OK, qv is KO). In such cases, assume there are m states $b_1, b_2, \cdots, b_m$. For each state

only certain symbols from the set $S_1, S_2, \cdots, S_n$ can be transmitted (different subsets for different states). The transmission of symbol S_k from state b_i to state b_j (b_i may be the same as b_j) takes time $t_{ij}^{(k)}$. This process is illustrated by a graph such as that shown in Fig. 4.15.
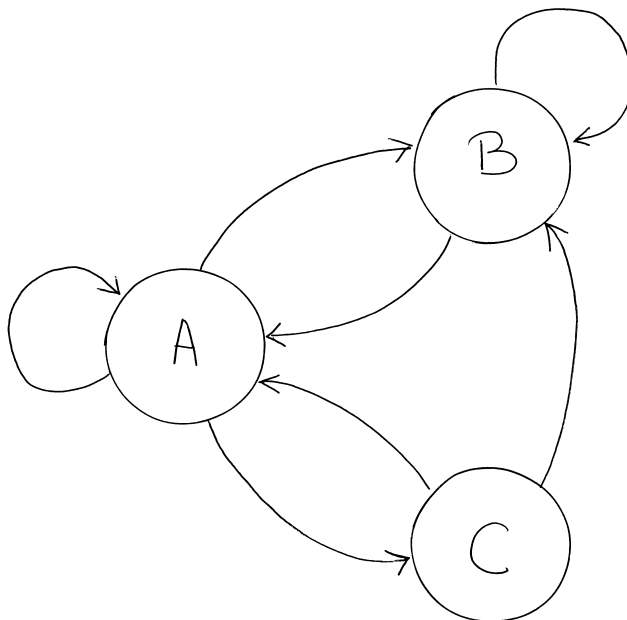
Figure 4.15: This graph describes the grammar in which the transitions $A \to (A, B, C)$, $B \to (A, B)$, and $C \to (A, B)$ are allowed. The transitions $B \to C$ and $C \to C$ are forbidden. Each word has a length independent of the transition $b_i \to b_j$.

Theorem: The channel capacity C is $\log X_0$, where X_0 is the largest real root of the $m \times m$ determinantal equation

$$\det \left| \sum_k X^{-t_{ij}^{(k)}} - \delta_{ij} \right| = 0 \tag{4.19}$$

Example: Assume the word A has length 2 and the words B and C have length 3 for the graph shown in Fig. 4.15. Assume the transmission time is proportional to the word length. Then the capacity of the channel in this figure is determined by solving the equation

$$\det \begin{bmatrix} \frac{1}{X^2} - 1 & \frac{1}{X^2} & \frac{1}{X^2} \\ \frac{1}{X^3} & \frac{1}{X^3} - 1 & 0 \\ \frac{1}{X^3} & \frac{1}{X^3} & -1 \end{bmatrix} = 0$$

so that $X_0 = 1.429108$ and $C = 0.357051$.

The table which effects the isomorphism between topological entropy for dynamical systems and channel capacity for communication systems is

Communication Systems	Dynamical Systems
graph	branched manifold
S_i	branch
t_i	period
b_j	branch line
channel capacity	topological entropy

In the following series of examples we compute the topological entropy for a number of dynamical systems using the result (4.18) or (4.19).

Example 1: Smale horseshoe template, all symbol sequences are allowed. Then $S_1 = 0$, $S_2 = 1$, $t_1 = t_2 = 1$, and (4.18) becomes

$$1 = \frac{1}{X} + \frac{1}{X}$$

The solution is $X_0 = 2$, $h_T = \log 2 = 0.693147$.

Example 2: Smale horseshoe template, all combinations of the symbol sequences 1 and 01 are allowed. Then $t_1 = 1$ and $t_2 = 2$, so (4.18) becomes

$$1 = \frac{1}{X} + \frac{1}{X^2}$$

The solution is $X_0 = \frac{1}{2}(1 + \sqrt{5})$, $h_T = 0.481212$.

Example 3: Smale horseshoe template again, only the symbol sequences 01, 011, 0111 and 01111 occur, but all combinations of these symbol sequences are allowed. Then (4.18) becomes

$$1 = \frac{1}{X^2} + \frac{1}{X^3} + \frac{1}{X^4} + \frac{1}{X^5}$$

The solution is $X_0 = 1.534158$, $h_T = 0.427982$.

Example 4: A branched manifold with m branches has an $m \times m$ Incidence Matrix I. Transit through each branch takes one period. Then (2) becomes

$$\det \left[\frac{1}{X} I_{ij} - \delta_{ij} \right] = X^{-m} \det \left[I_{ij} - X \delta_{ij} \right] = 0$$

As a result, in this case the topological entropy is the logarithm of the largest real eigenvalue of the Transition Matrix I.

4.10.3   Entropy and Mode Locking

The next series of examples deals with a standard route to chaos described by the standard model. In this case a nonlinear dynamical system first undergoes a Hopf bifurcation. The resulting torus become increasingly wrinkled. On the way to chaos mode locking first appears (analogous to period doubling), and then chaotic behavior occurs. Applying the Birman-Williams theorem to this scenario, we find that the branch line is not a segment of R^1 but rather the circle S^1. Mode locking occurs when the mapping $S^1 \to S^1$ is still invertible. When it loses invertibility, chaos appears.

Invertibility is lost when the circle folds over on itself during the return map. Because of the boundary conditions (S^1 is topologically different from R^1), two folds must occur. The flow from S^1 to its folded over image is described by a three branch manifold. Branches L and R are orientation-preserving. On branch L the rotation angle increases by less than 2π, on branch R it increases by more than 2π. Branch C occurs between the two folds and is orientation reversing.

Chaos appears when two Arnol'd tongues begin to overlap. Arnol'd tongues are described by rational fractions p/q, where q is the number of times the closed orbit goes around the torus in the long direction and p is the number of times it goes around in the short direction. Then q is the period and p is the winding number.

The symbol sequence of the saddle node pair in the Arnol'd tongue p/q is $W(1)W(2)\cdots W(q)$, where

$$W(i) = [i \times \frac{p}{q}] - [(i-1) \times \frac{p}{q}] = \left(\begin{array}{c} 0 \\ 1 \end{array} \right) \longrightarrow \left(\begin{array}{c} W(i) = L \\ W(i) = R \end{array} \right)$$

where $[x]$ is the integer part of x. For $p/q = 3/5$, $W(1)W(2)W(3)W(4)W(5) \to LRLRR$. The partner orbit is obtained by replacing the penultimate symbol by C (for example, $LRLCR$).

We describe the chaotic behavior when tongues described by rational fractions p/q and p'/q' begin to overlap, with $p/q < p'/q'$ and $pq' - p'q = \pm 1$. At this point the behavior is chaotic and the grammar contains three words. These are:

    A The symbol sequence for the left hand tongue p/q

    B The symbol sequence for the right hand tongue p'/q'

    C The partner of B

Not every symbol sequence is allowed, for C must be preceded by A.

Example 5: Determine the equation which defines the topological entropy for the chaotic attractor formed when the tongues p/q and p'/q' cross. The Transition Matrix is

$$\begin{array}{c} A \\ B \\ C \end{array} \quad \left[\begin{array}{ccc} 1 & 1 & 1 \\ 1 & 1 & 0 \\ 1 & 1 & 0 \end{array} \right]$$

Applying this information to Equ (4.19), we find

$$\det \left[\begin{array}{ccc} \frac{1}{X^q} - 1 & \frac{1}{X^q} & \frac{1}{X^q} \\ \frac{1}{X^{q'}} & \frac{1}{X^{q'}} - 1 & 0 \\ \frac{1}{X^{q'}} & \frac{1}{X^{q'}} & -1 \end{array} \right] = 0$$

This reduces to

$$X^{q+q'} - X^q - X^{q'} - 1 = 0$$

Example 6: Use Equ (4.18) to obtain the same result. Since A must proceed C, the grammar has three symbols A, B, and AC with periods q, q', and $q + q'$ and no constraints. The secular equation is

$$\frac{1}{X^q} + \frac{1}{X^{q'}} + \frac{1}{X^{q+q'}} = 1$$

which is equivalent to the result above.

Example 7: Compute the topological entropy for the strange attractors which occur when the tongues p/q and p'/q' just overlap, for the pairs $(\frac{1}{2}, \frac{2}{3})$, $(\frac{1}{2}, \frac{3}{5})$, $(\frac{3}{5}, \frac{2}{3})$. Solution:

p/q	p'/q'	A	B C	X_0	h_T
$\frac{1}{2}$	$\frac{2}{3}$	LR	LRR LCR	1.429108	0.357051
$\frac{1}{2}$	$\frac{3}{5}$	LR	$LRLRR$ $LRLCR$	1.307395	0.268037
$\frac{3}{5}$	$\frac{2}{3}$	$LRLRR$	LRR LCR	1.252073	0.224801

Example 8: Compute the topological entropy for the low period Arnol'd tongues for which $pq' - qp' = \pm 1$. Solution: To period ten, here they are. The entries for which q and q' have a common factor are left blank.

	3	4	5	6	7	8	9	10
2	0.357051		0.268037		0.219131		0.187366	
3		0.253442	0.224801		0.186002	0.172048		0.150507
4			0.196620	0.178525	0.164136		0.142458	0.134018
5				0.160664	0.148188	0.137920	0.129277	
6					0.135847	0.126721	0.119017	0.112400
7						0.117680	0.110713	0.104716
8							0.103803	0.098310
9								0.092856